Arabian Journal of Geosciences (2023) 16:129
https://doi.org/10.1007/s12517-023-11236-0

ORIGINAL PAPER

The presence of extensional volcanic basins along a transpressive bend: a case of extension-transpression co-existence from the Lebanese Restraining Bend

Tony S. Nemer[1]

Received: 24 October 2022 / Accepted: 24 January 2023 / Published online: 31 January 2023

Abstract
The Lebanese Restraining Bend is 170 km long and lies obliquely along the N-S trending Dead Sea Transform Fault, which is the continental plate boundary between Arabia and Africa. Of particular attention about the Lebanese Restraining Bend is the presence of two basins in its southern and northern bounds that are bordered by basalts; these are the Hula basin and the Bouqayaa basin, respectively. These two basins and the presence of basalts in their vicinities raise questions about (1) their locations in the immediate proximity to a transpressive bend, (2) the tectonic interrelation between the formation of the basins and the emplacement of the basalts, and (3) the timing of the formation of the basins relative to the prevailing regional transpression. In this paper, the author sheds light on these aspects and proposes a simplistic kinematic model of the tectonics behind the transpressive regime, the formation of the basins, and the emplacement of the basalts. The presented model highlights the tectonic interrelation between the formation of the basins, their bordering basalts, and the deformation of the transpressive bend. The regional strike-slip movements along the faults outside and within the transpressive bend seem to have caused co-existing extensional and compressional regimes, and they suggest that the formation of the basins may be contemporaneous with the regional transpression. The results can serve as a conceptual model for more advanced boundary-element modeling and finite-element modeling of the tectonics of the Lebanese Restraining Bend, with potential broader insight into the understanding of the tectonics of transpressive bends and their interrelation with adjacent extensional basins, worldwide.

Keywords Volcanic basin · Restraining bend · Transform fault · Lithospheric extension · Kinematic modeling

Introduction

The cause of basaltic intraplate volcanism is not very well understood. Numerous continental intraplate volcanics occur near rift systems, and lithospheric extension may lead to the generation of magmas in the upper mantle (McKenzie and Bickle 1988). The Arabian plate hosts several basaltic regions where magmas may have generated due to plume activity and lithospheric thinning (Krienitz et al. 2009; Fig. 1). Several models have been proposed to explain the northern Arabia volcanism. These include (1) northward moving of Afar mantle plume magma (e.g. Camp and Roobol 1992), (2) the melting of lithosphere by heat conduction from underlying anomalously hot mantle (e.g., Weinstein et al. 2006), (3) gradual lithospheric thinning and contact with asthenospheric sources (Stein and Hofmann 1992; Bertrand et al. 2003; Shaw et al. 2003; Lustrino and Sharkov 2006), and (4) rifting over a localized hot spot and asthenospheric uplift (Diner 2019).

The Dead Sea Transform Fault (DSTF) is the continental plate boundary between Arabia and Africa (Fig. 1). It is a left-lateral fault, about 1000 km long, and extends in a south-north direction from the Gulf of Aqaba in the Red Sea to southeast Turkey where it connects with the East Anatolian Fault in the Karasu Valley. Along its length, transtensional movement has led to the formation of several depressions and pull-apart basins (e.g. Mart 1991). These include the Dead Sea, the Hula basin, and the Ghab depression. In addition, other grabens are present like the one to the southwest

Responsible Editor: François Roure

✉ Tony S. Nemer
tn01@aub.edu.lb

[1] Department of Geology, American University of Beirut, P.O.Box 11-0236, Riad El-Solh, Beirut 1107 2020, Lebanon

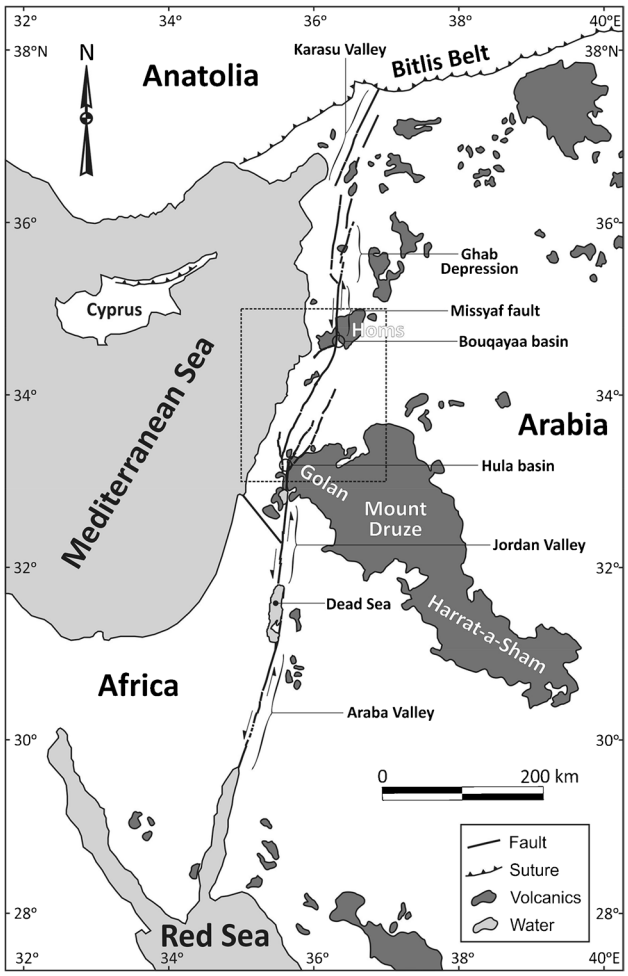

Fig. 1 Regional map of the eastern Mediterranean area showing the Dead Sea Transform Fault between Africa and Arabia, the Bitlis suture zone between Arabia and Anatolia, and the distribution of volcanics in the region. Box surrounds the Lebanese Restraining Bend and delineates the location of Fig. 2. Modified from Adiyaman and Chorowicz (2002)

of Golan, Mount Druze, and Harrat-a-Shamah volcanic field (Almond 1986; Brew et al. 2001; Fig. 1).

The DSTF bends rightward about midway its length where it forms a transpressive bend, known as the Lebanese Restraining Bend (LRB). Within the LRB, the DSTF splays into 4 major faults: Yammouneh, Roum, Rachaya, and Serghaya faults. All these faults have been proven active through paleoseismological and active tectonic investigations (e.g. Gomez et al. 2003; Daeron et al. 2005; Nemer and Meghraoui 2006; Nemer et al. 2008a, b; Nemer 2019; Fig. 2). The tectonic framework of the LRB involves a positive flower structure that hosts the different fault branches of the DSTF within the transpressive bend (Nemer and Meghraoui 2020). To the north of this bend, the DSTF resumes its south-north trend along the Missyaf fault and Ghab depression (Fig 1).

At the southern and northern bounds of the LRB lie two basins that are bordered by basaltic regions: these are the Hula basin and the Bouqayaa basin, respectively (Dubertret 1955, 1962; Figs. 1 and 2). The Hula basin lies at the northwestern edge of a large volcanic province that includes Golan, Mount Druze, and Harrat-a-Shamah. The Bouqayaa basin is bordered by the Homs basalts to the north of the restraining bend (Fig. 1).

The Golan, Mount Druze, and Harrat-a-Shamah volcanic province is the largest volcanic plateau of the Arabian plate. These basalts extend in a southeast direction from the southern bound of the LRB for more than 400 km (Weinstein et al. 2020; Fig. 1). They consist of dike-cut lava flows that include scoria cones (Krienitz et al. 2009), and reach a cumulative thickness of about 1500 m (e.g. Guba and Mustafa 1988). The Homs basalts extend in a northeast-southwest direction for about 75 km at the northern bound of the LRB (Fig. 1). They consist of a succession of lava flows with minor sills of about 200 m in cumulative thickness in the Akkar region, Lebanon (Abdel-Rahman and Nassar 2004), and reach up to 850 m in thickness in the Homs region, Syria where they are intercalated with pyroclastic deposits (Chorowicz et al. 2005).

The Hula and Bouqayaa basins and the presence of basalts around them raise questions about (1) their locations in the immediate proximity to the LRB, (2) the tectonic relation between their formations and the basalt emplacements, and (3) the relative timing of basin extension to regional transpression. In this paper, the author discusses these aspects and proposes a simplistic kinematic model of the tectonics behind this setting. The results help highlight the interrelation between the LRB and the formation of the nearby volcanic basins and provide a conceptual model for more advanced boundary-element modeling and finite-element modeling of the tectonics of this transpressive bend, which may serve as an example with broader implications on comparable tectonic systems, worldwide.

Tectonic setting

The volcanics of the southern and northern bounds of the LRB form two areas of Arabia's Cenozoic volcanic regions that extend from south and southwest Arabia, along the DSTF, to south of the Bitlis Belt in north Arabia (e.g., Abdel-Rahman and Kallas 2013; Fig. 1). The volcanics along the DSTF are Miocene to Holocene in age, with a phase of inactivity between 16 and 8.5 Ma (Mouty et al. 1992; Chorowicz et al. 2005). These volcanics are mostly within-plate basalts, and their occurrence was associated with the left lateral movement along the DSTF (e.g., Mouty et al. 1992). The Golan-Harrat-a-Shamah eruptions took place over three stages: at 26–22 Ma, 18–13 Ma, and 7 to <

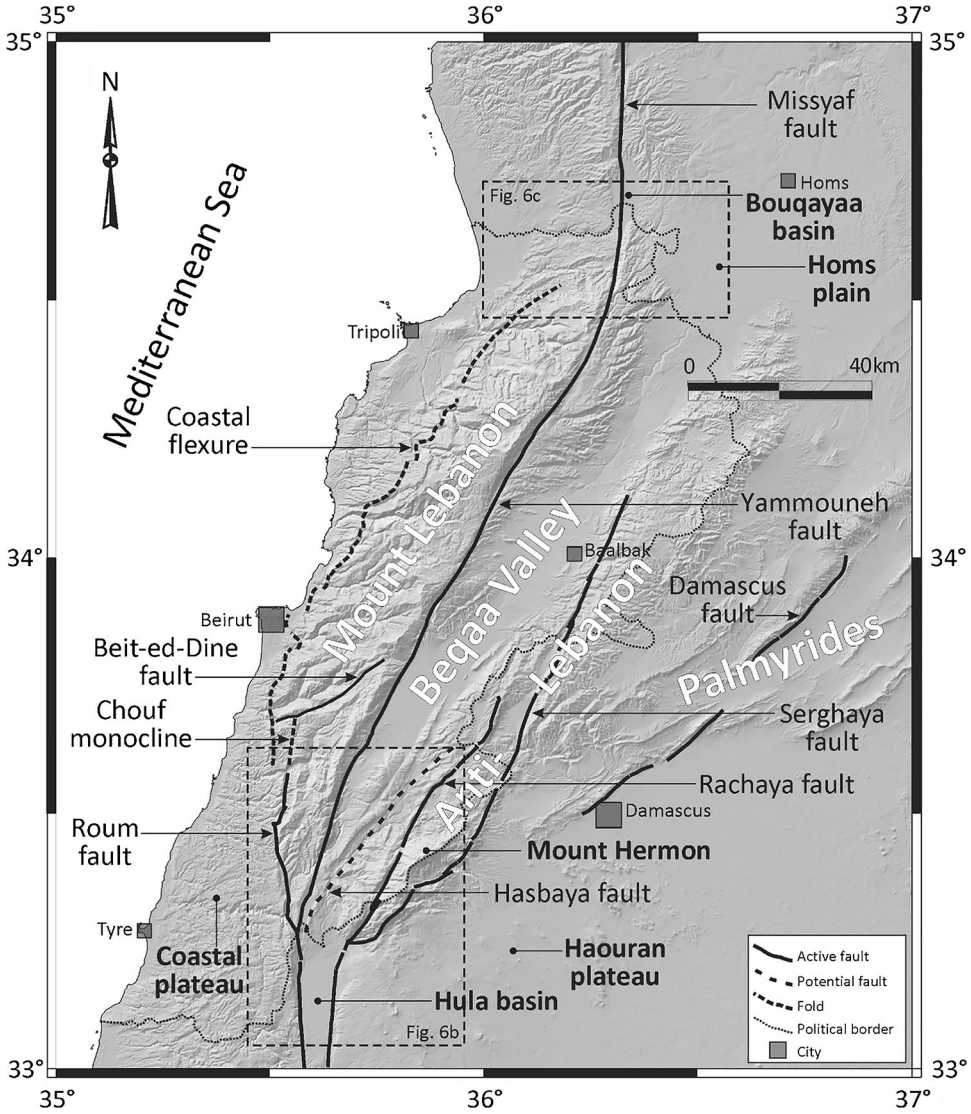

Fig. 2 Digital elevation model (SRTM, 90-m resolution) of the Lebanese Restraining Bend showing the main physiographic units and geological structures. Location is shown in Fig. 1. Boxes are locations of Figs. 6b and 6c

0.5 Ma (Chorowicz et al. 2005; Fig. 1). Mor (1993) reported K-Ar ages of the southern Golan basalts ranging from Lower Pliocene (5.0 to 3.5 Ma) to Upper Pleistocene (0.4 to 0.1 Ma), and of the northern Hula basin basalts ranging from 2.9 to 1.7 Ma. The Homs basalts are dated at 6.5–2.0 Ma (e.g., Mouty et al. 1992; Butler et al. 1997).

Garfunkel (1989) suggested that the "cover" basalts of the southern Golan are ocean island basalt (OIB) of intraplate character, and proposed that the Jordan Valley extensional fault could have been a path for magma expulsion (Fig. 1). Shaw et al. (2003) indicated that the basalts and basanites of Harrat-a-Shamah (Fig. 1) erupted as a result of lithospheric extension. Abdel-Rahman and Nassar (2004) indicated that the Pliocene lavas of the Homs basalts formed due to local extension by a small degree of partial melting of a primitive mantle source, and considered the DSTF to be active in Late Cenozoic during the eruption of those basalts. Lustrino and Sharkov (2006) suggested that the Neogene volcanism to the north of the LRB took place near the DSTF due to mantle decompression and the transition from transpressional to transtensional stresses (Fig. 1). Abdel-Rahman and Kallas (2013) provided a review of the mechanisms of the volcanic eruptions throughout the Arabian plate, and underlined that, rather than mantle plumes that have caused the East African Rift volcanism, decompression melting of the mantle associated with extension may represent a plausible process for Plio-Quaternary volcanism in the eastern Mediterranean region (Fig. 1).

Data and methodology

The following data were used and leveraged for the building of the model and the interpretation of the results: the existing geological maps of Lebanon and its surroundings (e.g., Dubertret 1955, 1962), the Shuttle Radar Topography

Mission 90-m digital elevation data, the available tectonic studies of the study area (e.g., Butler et al. 1997; Brew et al. 2001; Adiyaman and Chorowicz 2002; Chorowicz et al. 2005; Goren et al. 2015; Nemer and Meghraoui 2020), the active tectonic studies of the LRB (e.g., Gomez et al. 2003; Daeron et al. 2005; Nemer and Meghraoui 2006; Nemer et al. 2008a, b), available geodetic studies (e.g., Mor 1993; Gomez et al. 2007; Palano et al. 2013; Gomez et al. 2020), geochemical studies of the study area (e.g., Bertrand et al. 2003; Shaw et al. 2003; Abdel-Rahman and Nassar 2004; Weinstein et al. 2006; Abdel-Rahman and Kallas 2013), and gravity data (e.g., Rybakov et al. 2003; Schattner and Weinberger 2008).

The division of the modeled area into separate blocks bounded partially by faults required some constraints to define the blocks in order to (1) accommodate the block boundaries where minor or no faults/structures exist, (2) have a reasonable number of blocks to model, and (3) keep the modeling process simple by avoiding distortion of the modeled blocks. With this in mind, The LRB was divided into seven tectonic blocks based on the spatial distribution and tectonic behavior of the main structures (Fig. 3). Where no structures exist, the block boundaries were extended for the need to delimit the blocks in the model (Figs. 2 and 3): Block 1 is bounded by the eastern Hula basin fault, southern Serghaya, and southern Damascus faults. Block 2 is bounded by the Hula basin faults, Yammouneh, Missyaf, Rachaya, and Serghaya faults. Block 3 is bounded by the western Hula basin fault, Roum fault, coastal flexure, and Missyaf fault. Block 4 is bounded by the Rachaya and Serghaya faults. Block 5 is bounded by the Serghaya and southern Damascus faults. Block 6 is bounded by the Roum fault, Chouf monocline, Beit-ed-Dine, and Yammouneh faults. Block 7 is bounded by the coastal flexure, Beit-ed-Dine, and Yammouneh faults.

The model was based on a backward restoration of the different blocks from their present-day locations into a pre-existing phase, with each block having its own reference as its present-day location (Fig. 3). The restorations were performed as rigid body translations, with some minor rotations, but with no dilations, nor distortions. This simplistic approach relates directly to the two-dimensional nature of the modeling, which did not require recognizing the internal block deformations and the vertical component of deformation that are not thoroughly reflected in the model. Ideally, the restoration of each block should in a way revert the GPS-derived displacement vectors, assuming these vectors are representative of the long-term corresponding displacement amounts and rates (e.g., Gomez et al. 2007; Gomez et al. 2020). However, the potential division of each block into smaller blocks (e.g., Goren et al. 2015), the probable change in displacement rates, and the timing of movement of each block relative to its neighboring blocks, all rendered the restoration to be made with some limitations, including the matching with present-day geodetic data. In particular, the model mainly honored the strike-slip fault movements of the blocks, whereby the movements along the bounding faults were restored (Fig. 3b). The model accounted partly for the compression that is now manifested in folds, which was empirically restored into gaps between the blocks based on the two-dimensional nature of the restoration. Similarly, the model underwent some overlap of adjacent blocks in the pre-existing phase (Fig. 3b) only in places where presently

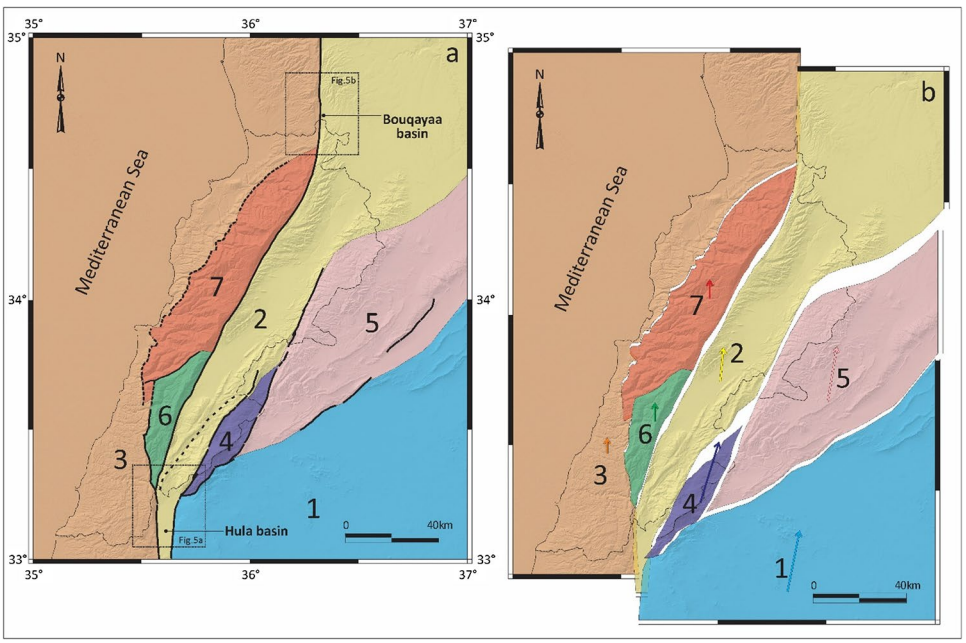

Fig. 3 **a** The study area divided into seven tectonic blocks (numbered) based on the structures shown in Fig. 2. **b** The tectonic blocks restored into a pre-existing phase (see text for details). The arrows in (**b**) represent the reversal of the restorations, and they are the displacement vectors of the corresponding blocks from the pre-existing tectonic phase (**b**) into the present-day phase (**a**)

(Fig. 3a) we have extensional basins and structures, such as in Hula and Bouqayaa basins.

As to the timing of block movements, it is important to note that it is not absolute, but relative or rather in relation to the adjacent blocks. In fact, an absolute timing of block movements would require knowledge of the differential slip rate of each of the bounding faults, together with the rate of uplift and subsidence in the different blocks. This would require more advanced numerical modeling that takes into account the timing of block movements, and the 3-dimensional change of the physiography, including erosion and sedimentation.

Lastly, it is very important to keep in mind the uncertainties and limitations of the applied modeling, namely: the 2-dimensional nature of the presented modeling, the matching of block movements with present-day geodetic data, the absolute timing of block movements, the differential slip rate of the bounding faults, the rate of uplift and subsidence of the modeled blocks, the internal deformation of the blocks (rotation, dilation, distortion), the 3-dimensional change of the physiography, and the change of fault activity/inactivity with time. In addition, concerning the fault plane solutions of the study area, several studies have been performed (e.g., Pondrelli et al., 2002; Salamon et al., 2003; Hofstetter et al., 2007; Abdul-Wahed et al., 2011; Meirova and Hofstetter, 2013; Palano et al., 2013), making available several mechanisms covering in part the LRB. However, as many of those mechanisms have different coordinates for the same events provided by different seismic catalogues, and as many other mechanisms lie away from the defined block boundaries, the author leveraged those mechanisms to generate synthetic mechanisms for the block-bounding structures, based on geological data, field observations, fault geometries, tectonic settings, and active tectonic data.

Modeling results

Following the above-mentioned settings, several restoration attempts were modeled, one of which is presented in Fig. 3b as a reasonable model that highlights the tectonic transition from the present-day tectonic phase (Fig. 3a) into a pre-existing phase (Fig. 3b).

Block 1 underwent translation to the south and southwest along its western and northern boundaries, respectively. This has led to some overlap with Block 2 in the east of the Hula basin, and gaps with Blocks 4 and 5.

Block 2 underwent translation to the south along the Hula basin and Missyaf faults, and translation to the SSW along the Yammouneh fault. This has led to some overlaps with Block 3 in the west of the Hula and Bouqayaa basins, some other overlaps with Blocks 1 and 4 in the east of the Hula basin, and gaps with Blocks 4, 5, 6, and 7.

Block 3 underwent translation to the south along the west Hula basin, Roum, and Missyaf faults. This has led to some overlap with Block 2 in the west of the Hula and Bouqayaa basins (mentioned above), some minor overlap with Block 6 along the southern segment of the Roum fault, a minor gap with Block 6 along the northern segment of the Roum fault, and some translation away from Block 7 along the trend of the coastal flexure.

Block 4 underwent translation to the southwest along the Rachaya and Serghaya faults, with minor clockwise rotation about its axis. This has led to a minor overlap with Block 2 to the east of the Hula basin (mentioned above), and to gaps with Blocks 1, 2, and 5.

Block 5 underwent translation to the WSW and southwest along its southern boundary and the Serghaya fault, respectively. This has led to gaps with Blocks 1, 2, and 4.

Block 6 underwent translation to the south along the Roum fault. This has led to some minor overlaps with Blocks 3 and 7 along the southern segment of the Roum and the Beit-ed-Dine faults, respectively. Also, it has led to a minor gap with Block 3 along the northern segment of the Roum fault, and to a gap with Block 2 (mentioned above).

Block 7 underwent translation to the south away from Block 3 towards Block 6. This has led to a minor overlap with Block 6 along the Beit-ed-Dine fault, to a gap with Block 3 along the trend of the coastal flexure, and to a gap with Block 2 (mentioned above).

Discussion

The modeled block movements and current physiography

The backward (inverse) modeling presented above (Fig. 3b) has proved very useful in explaining the tectonic interrelation between the current blocks (Fig. 3a) and the various physiographic units of the LRB, including the Hula and Bouqayaa basins (Fig. 4). In effect, as Block 1 has moved NNE from a pre-existing position (Fig. 3b) into the present position (Fig. 3a), the overlap with Block 2 has transformed into extension along the eastern margin of the Hula basin, and the gaps led to compression with Block 4 (south Mount Hermon) and Block 5 (southwest Palmyrides; Fig. 4). Similarly, Block 2 has moved NNE into its current position, and the overlaps with Block 3 have transformed into extensions in the Hula and Bouqayaa basins, and the gaps have led to compression with Block 4 (north Mount Hermon), Block 5 (north Anti-Lebanon), and Blocks 6 and 7 (Mount Lebanon). Block 3 has moved north into its present position: in addition to the overlaps with Block 2 (mentioned above), the minor overlap and gap with Block 6 have led to the extensional

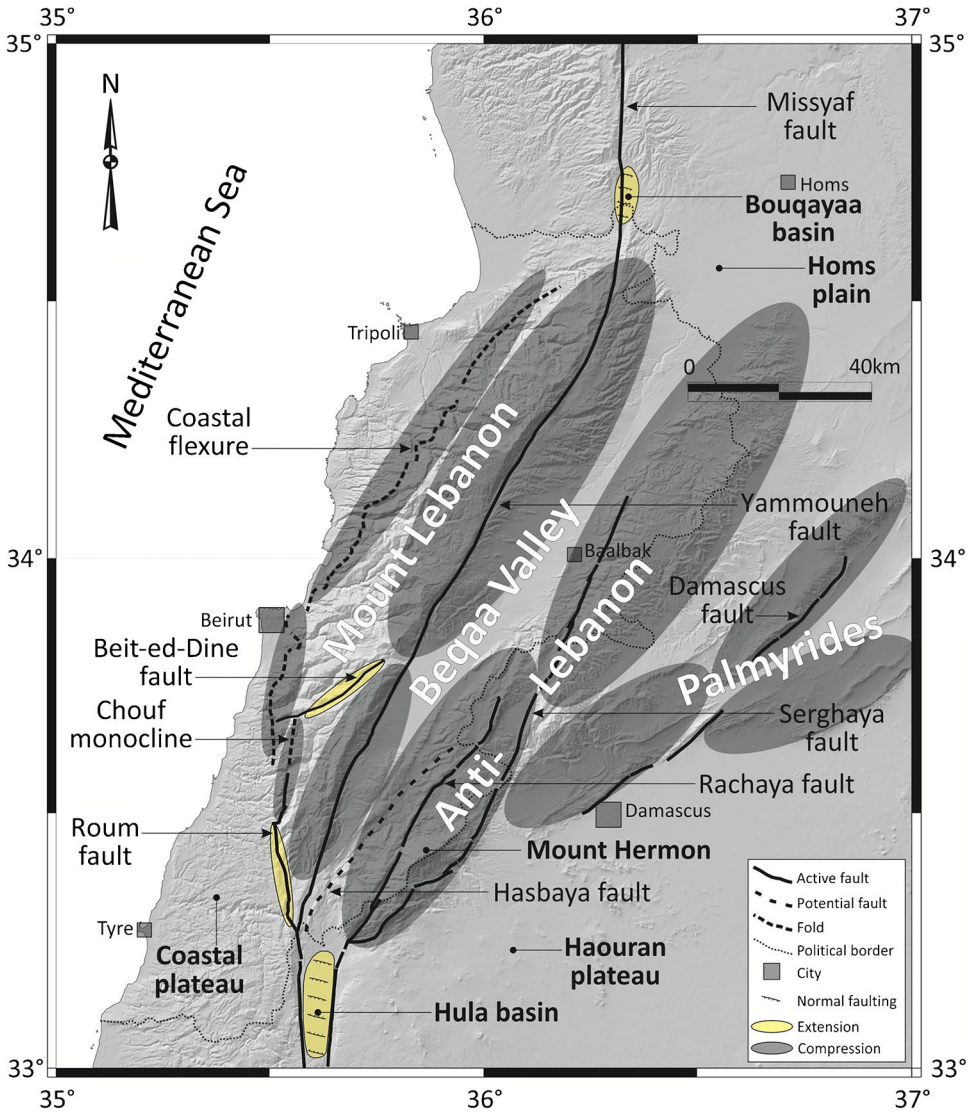

Fig. 4 Digital elevation model (SRTM, 90-m resolution) of the Lebanese Restraining Bend showing the present tectonic phase with the zones of compression (dark gray) and extension (yellow) as detected from the kinematic modeling shown in Fig. 3

and compressional components of the southern and northern segments of the Roum fault, respectively (Nemer and Meghraoui 2006), and the gap with Block 7 has led to the compression along the coastal flexure. Block 4 has moved NNE, and the gaps around it have transformed into compression within Mount Hermon and around south Anti-Lebanon and southwest Palmyrides. Block 5 has moved NNE, and the gaps around it have transformed into compression in Anti-Lebanon and southwest Palmyrides. Block 6 has moved north: in addition to the minor overlap and gap with Block 3 (mentioned above), the overlap with Block 7 has transformed into extension along the Beit-ed-Dine fault. Block 7 has moved north: as mentioned above, the minor overlap with Block 6 has led to the extension along the Beit-ed-Dine fault, and the gap with Block 3 has transformed into the compression along the coastal flexure.

The Hula and Bouqayaa basins

The current tectonic configuration of the LRB is shown in Fig. 4 where, per the modeling presented above, compression is revealed mostly everywhere in the transpressive bend except (1) in Hula and Bouqayaa basins, (2) along the southern segment of the Roum fault, and (3) along the Beit-ed-Dine fault. The arrows in Fig. 3b are displacement vectors that represent the rigid body translation of each block from its pre-existing location into its present-day location, again with some minor rotations, but with no dilation, nor distortion, nor erosion, nor sedimentation. In other words, the modeling adapted a plate-driven approach whereby the deformations are concentrated along the plate boundaries and are caused by plate movement.

The Hula basin is delimited by the Hula western and eastern faults, while the Bouqayaa basin is crossed by the

Missyaf fault (Figs. 3 and 4). From the presented model, the relative displacements of the adjacent blocks in the two basins can be resolved into relative displacement vectors (Fig. 5). For instance, in the Hula basin, Block 1 underwent translation from south to north along the light blue vector oriented N11°E, and Block 2 underwent translation from south to north along the yellow vector oriented N5°E (Fig. 3b). So the displacement of Blocks 1 and 2 relative to each other is represented by the resultant black vector B1–B2 (Fig. 5a). Similarly, Block 4 underwent translation from south to north along the dark blue vector oriented N15°E, and Block 3 underwent translation from south to north along the orange vector oriented N (Fig. 3b); the displacement of Blocks 2 and 4 relative to each other is represented by the resultant black vector B2–B4, and the displacement of Blocks 2 and 3 relative to each other is represented by the resultant black vector B2–B3 (Fig. 5a). As to the Bouqayaa basin, the displacement of Blocks 2 and 3 relative to each other is also represented by the resultant black vector B2–B3 (Fig. 5b).

Based on the above, in the Hula basin, the relative displacements of Blocks 1–2, 2–3, and 2–4 have resulted in extensional displacements within the basin (Fig. 5a). In effect, as Blocks 1, 2, 3, and 4 have moved into their respective present-day positions, the tectonic setting of the Hula basin has been dominated by NNE-trending extension (Figs. 3b and 5a). This model-based result matches the gravity maps of Rybakov et al. (2003) and the seismic-reflection results of Schattner and Weinberger (2008) whereby NW-striking faults are depicted to be controlling the pull-apart growth of the Hula basin. Similarly, in the Bouqayaa basin, the relative displacements of Blocks 2–3 have also resulted in NNE-trending extension (Figs. 3b and 5b), which matches the results of Chorowicz et al. (2005) who reported NW-striking tension fractures that "fed the Shin volcano" to the north of the Bouqayaa basin. These extensional settings could relate to lithospheric extension and subsequent magma ascent and flows of within-plate basalts in the vicinity of the Hula basin and further southeast, as well as in and around the Bouqayaa basin (e.g., McKenzie and Bickle 1988; Shaw et al. 2003; Krienitz et al. 2009; Fig. 1). In effect, the within-plate geochemical characteristics of the basalts were reported in Abdel-Rahman and Nassar (2004) and Abdel-Rahman and Kallas (2013) based on Zirconium (Zr) and Yttrium (Y) measurements (Zr vs Zr/Y; Fig. 6).

The modeling results presented above suggest that the Hula and Bouqayaa basins have formed in extensional settings that are directly related to the tectonic block movements within the LRB. The combined strike-slip movements along the SN- and NNE-striking faults are hereby proposed to have led to the simultaneous compression (within the bend) and extension (at the southern and northern bounds of the bend; Fig. 7). In effect, the strike-slip movement along the Yammouneh fault is modeled to relate to and connect the extensional movements in the Hula and Bouqayaa basins. The strike-slip movement along the Rachaya-Serghaya faults is modeled to transform the extension in the Hula basin to the compression that is manifested in the Palmyride fold belt (e.g. Palano et al. 2013; Gomez et al. 2020). The strike-slip movements along the Hula faults are modeled to have led to the compressions that are manifested in the folds of Mount Lebanon and Anti-Lebanon. The strike-slip movement along the Bouqayaa fault is modeled to have also caused compression within Mount Lebanon (Fig. 7).

The resulting extensional settings of the Hula and Bouqayaa basins are hereby proposed to potentially be the

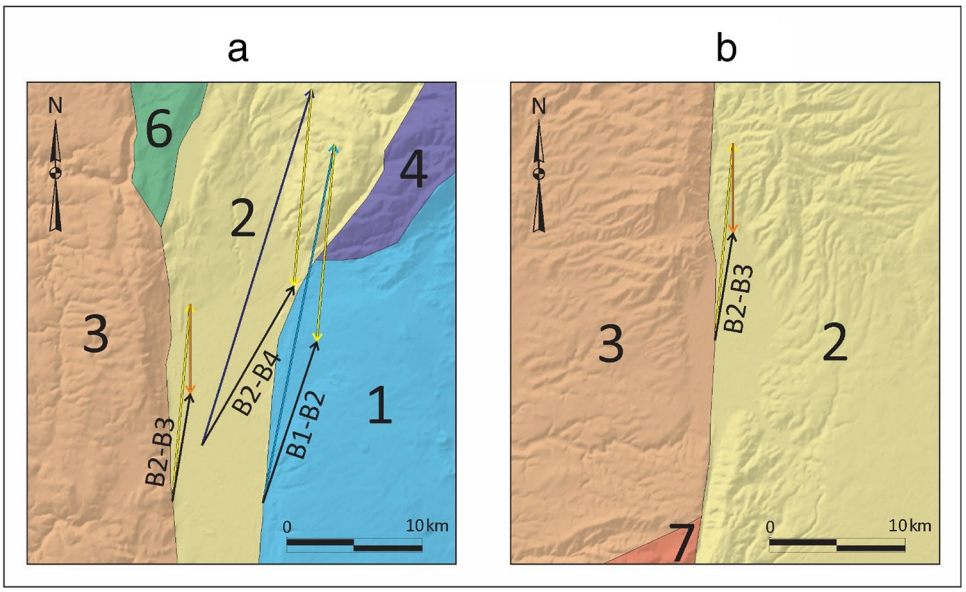

Fig. 5 The resulting displacement vectors (Fig. 3b) of Blocks 1–2, 2–3, and 2–4 taken in pairs in the Hula basin (**a**), and of Blocks 2-3 in the Bouqayaa basin (**b**). *B#-B#* = block pair. The colored vectors represent the relative displacement of the corresponding blocks (by color, Fig. 3b), and the black vectors are the resultants of each labeled pair (see text for details). Locations are shown in Fig. 3a

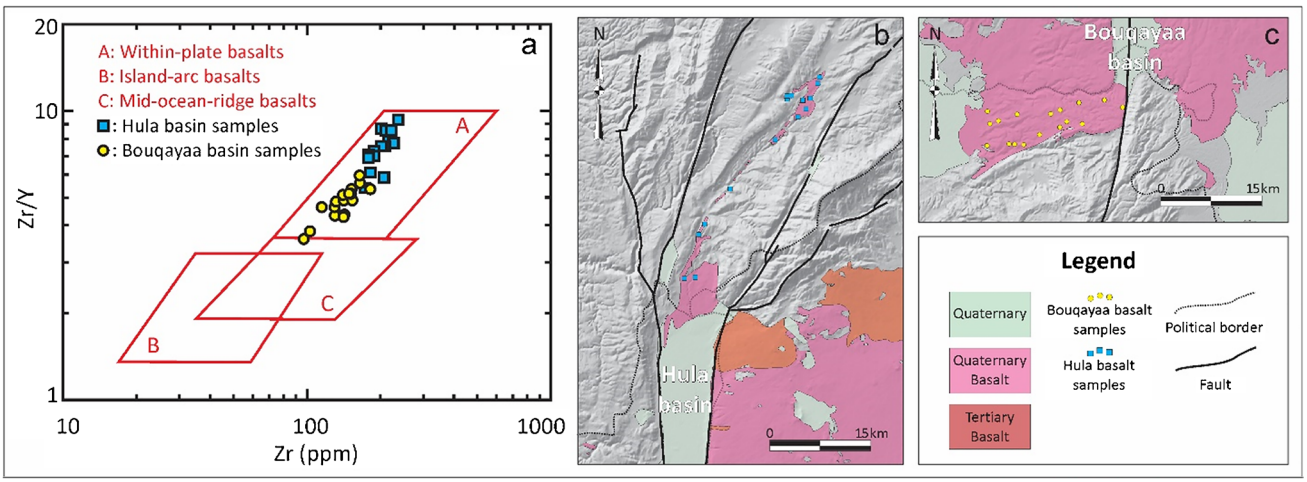

Fig. 6 **a** Zr vs Zr/Y variation diagram (Pearce and Norry 1979) for the Hula basalts (blue squares, locations in **b**) and Bouqayaa basalts (yellow circles, locations in **c**) after Abdel-Rahman and Kallas (2013) and Abdel-Rahman and Nassar (2004), respectively. Both types of basalts lie in box A, indicating within-plate basalts

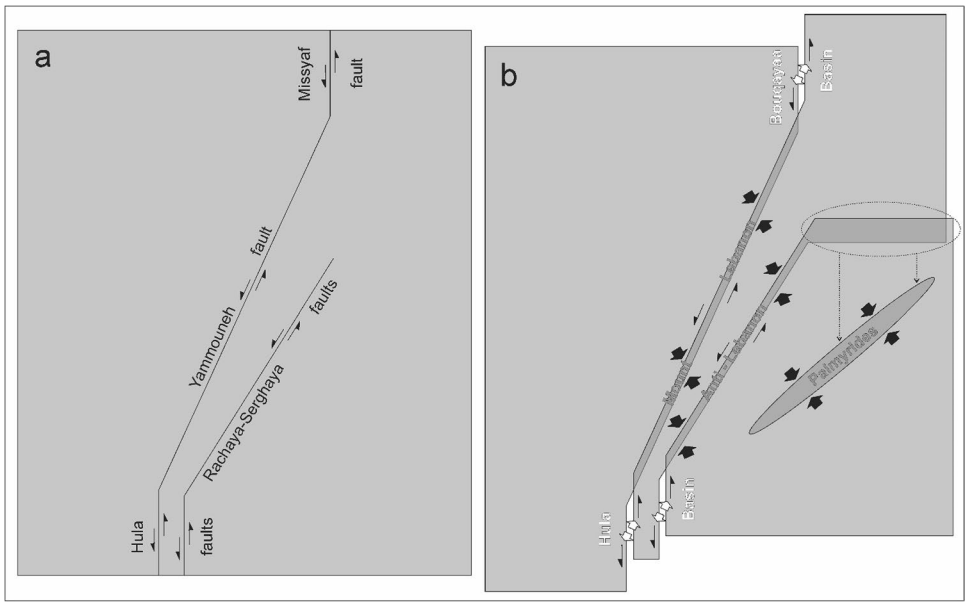

Fig. 7 Simplistic model of the movements along the main faults of the Lebanese Restraining Bend in the pre-movement (**a**) and post-movement (**b**) settings (cf. Figs. 2 and 4). In the pre-movement setting, only the strike-slip components of the faults are shown. In the post-movement setting: extension = diverging white arrows, compression = converging black arrows (see text for details)

causes of lithospheric extension and basaltic extrusions in the southern and northern bounds of the LRB, which may serve as an example with broader implications on comparable tectonic settings worldwide, such as the tectonics of Salton Trough basin close to California's Big Bend (e.g., Lachenbruch et al. 1985), and New Zealand's North Island volcanism near the Alpine Fault bend (e.g., Norris and Toy 2014). However, it should be noted that the presented modeling does not imply that the volcanic activities in the vicinities of the DSTF were restricted only to the Hula and Bouqayaa basins, as a result of the rightward bending of the left-lateral plate boundary. In fact, the documented "volcanic periodicity" during the last 5 Ma along the DSTF and the migration of the volcanic activity since the Pleistocene from the Hula basin eastward both suggest that the plate boundary acted as a pathway and a barrier for magma expulsion at different times, due to the fluctuations in the regional stress fields along the plate boundary itself (e.g., Weinstein et al. 2020).

Although the co-existence of compressional and extensional regimes may sound familiar when it comes to the distribution of regional stresses, the modeled interconnection between a restraining bend and its bounding extensional basins through strike-slip faulting is not something that is very well known. In fact, this is a concept that is definitely worth exploring further and in more detail, along the DSTF

and other plate boundaries, in order to understand the implications of having lithospheric extension in transpressional domains, as this may lead to additional insight into comprehending the origin of some volcanic activities in specific unusual places, such as the LRB.

Conclusion

A kinematic examination of the movement of the main tectonic blocks within the LRB offered valuable insight into the presence of extensional volcanic basins in the southern and northern bounds of the transpressive bend. The presented modeling highlighted the tectonic interrelation between the formation of the Hula and Bouqayaa basins, the emplacement of their bordering basalts, and the tectonics of the transpressive bend. The regional strike-slip movements along the SN- and NNE-striking faults, outside and within the LRB, may have led to co-existing extensional and compressional tectonic regimes, which suggests that the formation of the basins may be contemporaneous with the regional transpression. The model-based results match the present physiographic units of the LRB and are supported by the gravity and seismic-reflection results along the Hula basin (Rybakov et al. 2003; Schattner and Weinberger 2008) and by the structural and tectonic observations along the Bouqayaa basin (Chorowicz et al. 2005). The modeled extensional settings along the two basins are suggested to be the causes of lithospheric extension and subsequent magma ascent and flows of geochemically characterized within-plate basalts (Abdel-Rahman and Nassar 2004; Abdel-Rahman and Kallas 2013) at the southern and northern bounds of the LRB.

Acknowledgements This research was supported by a seed grant from the American University of Beirut, Lebanon. A. Abdel-Rahman is thanked for valuable discussions. Editor-in-Chief Al-Amri, Editor Roure, and two reviewers are thanked for their helpful reviews and suggestions that improved the manuscript.

Declarations

Conflict of interest The author declares that he has no competing interests.

References

Abdel-Rahman AM, Kallas LM (2013) Insights from the basalts of SE Lebanon into the nature of the Middle East Cenozoic volcanic province. Neues Jahrb Geol Palaontol Abh 270(2):209–232

Abdel-Rahman AM, Nassar PE (2004) Cenozoic volcanism in the Middle East: petrogenesis of alkali basalts from northern Lebanon. Geol Mag 141:545–563

Abdul-Wahed K, Asfahani J, Al-Tahhan I (2011) A combined methodology of multiplet and composite focal mechanism techniques for identifying seismologically active zones in Syria. Acta Geophysica 59(5):967–992

Adiyaman O, Chorowicz J (2002) Late Cenozoic tectonics and volcanism in the northwestern corner of the Arabian plate: a consequence of the strike-slip Dead Sea fault zone and the lateral escape of Anatolia. J Volcanol Geotherm Res 117:327–345

Almond DC (1986) Geological evolution of the Afro-Arabian Dome. Tectonophysics 131:301–332

Bertrand H, Chazot G, Blichert-Toft J, Thoral S (2003) Implications of widespread high-μ volcanism on the Arabian Plate for Afar mantle plume and lithosphere composition. Chem Geol 198:47–61

Brew G, Barazangi M, Al-Maleh AK, Sawaf T (2001) Tectonic and geologic evolution of Syria. GeoArabia 6:573–616

Butler RW, Spencer S, Griffiths HM (1997) Transcurrent fault activity on the Dead Sea Transform in Lebanon and its implications for plate tectonics and seismic hazard. J Geol Soc Lond 154:757–760

Camp VE, Roobol MJ (1992) Upwelling asthenosphere beneath western Arabia and its regional implications. J Geophys Res 97B:15255–15271

Chorowicz J, Dhont D, Ammar O, Rukieh M, Bilal A (2005) Tectonics of the Pliocene Homs basalts (Syria) and implications for the Dead Sea Fault Zone activity. J Geol Soc Lond 162:259–271

Daeron M, Klinger Y, Tapponnier P, Elias A, Jacques E, Sursock A (2005) Sources of the large A. D. 1202 and 1759 Near East earthquakes. Geology 33:529–532

Diner J (2019) Failed rifting in Jordan and the development of the Dead Sea Transform. J Geodyn 124:104–118. https://doi.org/10.1016/j.jog.2019.01.013

Dubertret L (1955) Carte géologique du Liban au 1:200,000 avec notice explicative. République Libanaise, Ministère des travaux publics

Dubertret L (1962) Carte géologique du Liban, Syrie, et bordure des pays voisins au 1:1,000,000. Muséum National d'Histoire Naturelle, Paris

Garfunkel Z (1989) Tectonic setting of Phanerozoic magmatism in Israel. Isr J Earth Sci 38:51–74

Gomez F, Meghraoui M, Darkal AN, Hijazi F, Mouty M, Suleiman Y, Sbeinati R, Darawcheh R, Al-Ghazzi R, Barazangi M (2003) Holocene faulting and earthquake recurrence along the Serghaya branch of the Dead Sea fault system in Syria and Lebanon. Geophys J Int 153:658–674

Gomez F, Karam G, Khawlie M, McClusky S, Vernant P, Reilinger R, Jaafar R, Tabet C, Khair K, Barazangi M (2007) Global Positioning System measurements of strain accumulation and slip transfer through the restraining bend along the Dead Sea fault system in Lebanon. Geophys J Int 168:1021–1028

Gomez F, Cochran WJ, Yassminh R, Jaafar R, Reilinger R, Floyd M, King RW, Barazangi M (2020) Fragmentation of the Sinai Plate indicated by spatial variation in present-day slip rate along the Dead Sea Fault System. Geophys J Int 221:1913–1940

Goren L, Castelltort S, Klinger Y (2015) Modes and rates of horizontal deformation from rotated river basins: application to the Dead Sea fault system in Lebanon. Geology 43(9):843–846. https://doi.org/10.1130/G36841.1

Guba I, Mustafa H (1988) Structural control of young basaltic fissure eruptions in the plateau basalt area of the Arabian Plate, northeastern Jordan. J Volcanol Geotherm Res 35:319–334

Hofstetter R, Klinger Y, Amrat AQ, Rivera L, Dorbath L (2007) Stress tensor and focal mechanisms along the Dead Sea fault and related structural elements based on seismological data. Tectonophysics 429:165–181

Krienitz MS, Haase KM, Mezger K, van den Bogaard P, Thiemann V, Shaikh-Mashail MA (2009) Tectonic events, continental intraplate volcanism, and mantle plume activity in northern Arabia: constraints from geochemistry and Ar-Ar dating of Syrian lavas. Geochem Geophys Geosyst 10(4):1–26

Lachenbruch AH, Sass JH, Galnis SP Jr (1985) Heat flow in southernmost California and the origin of the Salton Trough. J Geophys Res Solid Earth 90(B8):6709–6736. https://doi.org/10.1029/JB090iB08p06709

Lustrino M, Sharkov E (2006) Neogene volcanic activity of western Syria and its relationship with Arabian plate kinematics. J Geodyn 42:115–139

Mart Y (1991) The Dead Sea Rift: from continental rift to incipient ocean. Tectonophysics 197:155–179

McKenzie D, Bickle MJ (1988) The volume and composition of melt generated by extension of the lithosphere. J Petrol 29(3):625–679

Meirova T, Hofstetter R (2013) Observations of seismic activity in Southern Lebanon. J Seismol 17:629–644

Mor D (1993) A timetable for the Levant Volcanic Province, according to K-Ar dating in the Golan Heights. Israel Journal of African Earth Sciences 16(3):223–234

Mouty M, Delaloye M, Fontignie D, Piskin O, Wagner JJ (1992) The volcanic activity in Syria and Lebanon between Jurassic and Actual. Schweiz Mineral Petrogr Mitt 72:91–105

Weinstein Y, Nuriel P, Inbar M, Jicha BR, Weinberger R (2020) Impact of the Dead Sea Transform kinematics on adjacent volcanic activity. Tectonics 39:e2019TC005645. https://doi.org/10.1029/2019TC005645

Nemer TS (2019) The Bisri dam project: a dam on the seismogenic Roum fault, Lebanon Engineering Geology 261(2019) 105270. https://doi.org/https://doi.org/10.1016/j.enggeo.2019.105270

Nemer T (2020) Meghraoui M (2020) A non-active fault within an active restraining bend: the case of the Hasbaya fault. Lebanon J Struct Geol 136:104060. https://doi.org/10.1016/j.jsg.2020.104060

Weinstein Y, Navon O, Altherr R, Stein M (2006) The role of lithospheric mantle heterogeneity in the generation of Plio-Pleistocene alkali basaltic suites from Harrat Ash Shaam (Israel). J Petrol 47:1017–1050

Nemer T, Meghraoui M (2006) Evidence of coseismic ruptures along the Roum fault (Lebanon): a possible source for the AD 1837 earthquake. J Struct Geol 28:1483–1495

Nemer T, Meghraoui M, Khair K (2008a) The Rachaya-Serghaya fault system (Lebanon). Evidence of Coseismic ruptures and the AD 1759 earthquake sequence. J Geophys Res 113 B05312. https://doi.org/10.1029/2007JB005090

Nemer T, Gomez F, Al Haddad S, Tabet C (2008b) Coseismic growth of sedimentary basins along the Yammouneh strike-slip fault (Lebanon). Geophys J Int 175(3):1023–1039. https://doi.org/10.1111/j.1365-246X.2008.03889.x

Norris RJ, Toy VG (2014) Continental transforms: a view from the Alpine Fault. J Struct Geol 64:3–31. https://doi.org/10.1016/j.jsg.2014.03.003

Palano M, Imprescia P, Gresta S (2013) Current stress and strain-rate fields across the Dead Sea Fault System: constraints from seismological data and GPS observations. Earth Planet Sci Lett 369-370:305–316

Pearce JA, Norry MJ (1979) Petrogenetic implications of Ti, Zr, Y, and Nb variations in volcanic rocks. Contrib Mineral Petrol 69:33–47

Pondrelli S, Morelli A, Ekström G, Mazza S, Boschi E, Dziewonski AM (2002) European-Mediterranean regional centroid-moment tensors: 1997-2000. Phys Earth Planet Inter 130:71–101

Rybakov M, Fleischer L, ten Brink U (2003) The Hula Valley subsurface structure inferred from gravity data. Isr J Earth Sci 52:113–122

Salamon A, Hofstetter A, Garfunkel Z, Ron H (2003) Seismotectonics of the Sinai subplate - the eastern Mediterranean region. Geophys J Int 155:149–173

Schattner U, Weinberger R (2008) A mid-Pleistocene deformation transition in the Hula basin, northern Israel: implications for the tectonic evolution of the Dead Sea Fault. Geochem Geophys Geosyst 9(7):1–18

Shaw JE, Baker JA, Menzies MA, Thirlwall MF, Ibrahim KM (2003) Petrogenesis of the largest intraplate volcanic field on the Arabian Plate (Jordan): a mixed lithosphere-asthenosphere source activated by lithospheric extension. J Petrol 44(9):1657–1679

Stein M, Hofmann AW (1992) Fossil plume head beneath the Arabian lithosphere? Earth Planet Sci Lett 114:193–209